Experimental Investigations of Instrumented Fully Grouted Rock Bolts under Pull Load

Jemishkumar Modi
Department Mining Engineering, Indian Institute of Technology Kharagpur, Kharagpur, India

Debasis Deb
Department Mining Engineering, Indian Institute of Technology Kharagpur, Kharagpur, India

Rakesh Kumar
Department Mining Engineering, Indian Institute of Technology Kharagpur, Kharagpur India

ABSTRACT: Rebar-type rock bolts of 22 mm and a length of 600 mm are instrumented with four resistance strain gauges along the length. A total of 450 mm bolt lengths is embedded with resin grouted inside a cement mortar cast cylindrical sample of diameter 250 mm. Strain gauges are placed on the surface of the rod at four locations. The diameter of the hole is varied as 32 mm, 36mm, and 42 mm. The bolt is embedded cement mortar samples are placed in a pull-testing machine and firmly fixed on the frame by tie-rods. The rod is pulled with three different loading groups of rates. This paper analyzes load-deformation relationship curves for different hole diameters of pulling to observe the variation in peak bond strength and stiffness. The tensile strains obtained at four locations are validated with an analytical equation are in the paper.

Keywords: Fully grouted rock-bolt, pull-out tests, bond strength, bond stiffness, axial strain.

1 INTRODUCTION

Rock bolt is the key reinforcement member used to provide support to rock strata in tunnels, underground mine drives/galleries and other excavations. A bolt enhances mechanical properties of rock masses and reduce deformation and support time (Pinazzi et al., 2020). A fully grouted rock bolt generates shear stress along the interfaces of grout-bolt and grout-rock and resist the movement of rock by increasing overall stiffness of the bolted zone (Cai et al., 2004; Deb & Das, 2010). Every year millions of rock bolts are installed worldwide to support and stabilize engineering structures (Benmokrane et al., 1995).

On other hand, mechanics of shearing along the interfaces of bolt-grout-rock due to pull load was investigated by few researchers. These studies showed that in the absence of rock movement, shear strain along the bolt rod varies non-linearly having the maximum value at the load side and near zero value at the other end (Farmer, 1975). Li & Stillborg, 1999 showed the similar distribution of strain development on the bolt rod considering the deformation of rock. Since then several researchers attempted to simulate the shearing mechanism of bolt-grout and grout-rock interfaces using experimental and numerical models. Significant contribution was made to understand and evaluate the mechanism of bolt-grout interfaces (Hyett et al., 1996). Moreover,

extended finite element method (XFEM) were also proposed for analyzing the behavior of grouted rock bolts and applied for simulating reinforcement around tunnels and slopes (Deb and Gujjala, 2018). In the field, Short Encapsulation Pull Tests (SEPT) tests were performed by Pile et al., 2003 and Chugh et al., 2016 to determine anchorage test and optimize roof support systems.This experimental study evaluated the effects of grout types, hole diameter and rate of loading on bond strength, stiffness and distribution of axial strains along the bolt rod. The analytical and solution of displacement and strain proposed by Farmer, 1975 modified to fit the experimental data. Laboratory pull-out tests of instrumented bolts

For pull-out test, 22 mm TMT rebar bolts were imbedded into cylindrical concrete mortar samples. Pourable resin and catalyst without sand particles resin were used as the grout materials. The bolt shank was grouted inside cement mortar concrete samples. The hole diameter and loading rate were also varied to determine the load-deformation relationships.

1.1 Preparation of Pull-out Test Samples

Laboratory pull-out tests used concrete-prepared cylindrical samples. Cement, sand, and aggregate were mixed 1:1:2. The cement: water ratio was 1:0.5. A motorized concrete mixer was used to mix the above components for 20 minutes. Each mould measured 500 mm in length and 250 mm in diameter. Then a PVC pipe of 450 mm in length and diameter of 32 mm, 36 mm, or 42 mm were inserted into the mould. These pipes were placed in the centre of the mould to create a hole in the concrete samples while pouring the rest of the mixture. The remaining 450 mm height of the mould was filled with concrete so that no concrete mix entered the small diameter pipe. The small diameter pipe was removed after an hour of concrete filling the mould. The concrete sample was removed from the mould and cured in water for 28 days. To determine mechanical characteristics, NX-size concrete mix samples were also prepared.

1.2 Preparation of Instrumented Rock Bolts and Pasting of Strain Gauges

Four strain gauge were placed to each rod at predefined locations of 50 mm, 160 mm, 280 mm, and 390 mm from the bolt rod's top end (loading end). Since each strain gauge had 4 lead wires, a channel of 4 mm depth cut along the bolt length to accommodate 16 wires. Four slots of each having 2 cm axial and 8 mm length were cut for pasting the strain gauges. In this study, strain gauges of 350 ohms were used to measure the change of strain while pull load was applied gradually. Strain gauges have a gauge factor of 2.12.

Initially, grout material was poured annulus volume in the hole and immediately, the instrumented bolt was pushed manually inside the hole because not to disturb the connections between the strain gauges and the lead wires.

2 PULL-OUT TEST MACHINE WITH DATA ACQUISITION AND STORAGE

A pull-out testing machine has been fabricated as shown the Figure 1. During experiments, 10 tie rods were firmly tightened using nuts and washers so the sample and upper and lower plate could not move in any direction during loading. All data of linear variable differential transformer (LVDT) and strain gauges were logged in a data logger and stored in the computer as every 10 seconds.

3.1 Shear Load versus Shear Deformation

Load-deformation data of 09 samples were analyzed to determine the peak shear load (P) and the corresponding shear displacement (u_p). From the physical observations of the sheared samples, it was found that the dominating shearing surface could be either grout-rock interface since resin come out along with the bolt. The bond strength at bolt-grout interface was estimated using equation 2, considering an embedded length (L) of 450 mm and peak load, (P) and given in

Table 1. In this study, average bond stiffness was calculated for peak displacement u_p. Further values σ_b and κ are analysed to evaluate the relationship with hole diameter and grout type. At the end, analysis results of axial strains are also enumerated for different conditions and compared with analytical estimates.

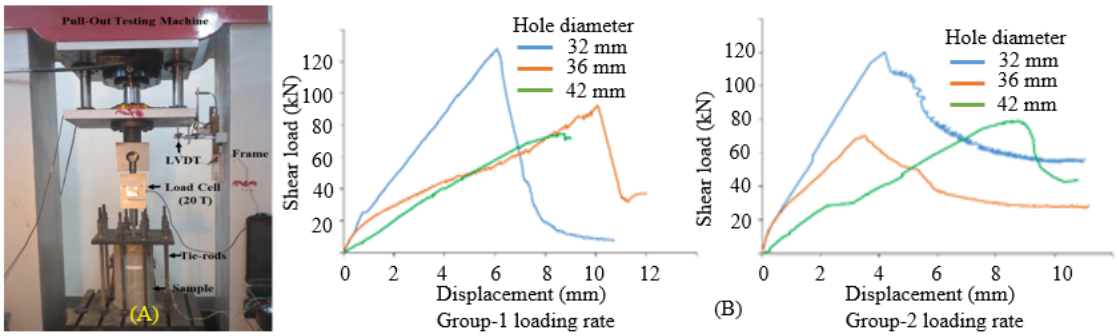

Figure 1(A). Pull-out Testing Machine and Figure 1(B). Shear load versus shear displacement plot of resin grouted sample.

The loading rate is categorized in 3 groups viz. Group-1: 60 to 80 µm/min, Group-2: 160 to 200 µm/min and Group-3: 230 to 280 µm/min. On average, the ratio of loading rates of Group-2 and Group-3 with respect to that of Group-1 are kept as 2.5 and 4.0, respectively. In this paper, a sample ID of 32RG1 refers to hole diameter of 32 mm, resin grouted and pulled by Group – 1 loading rate and so on.

2.1 Bond Strength

It has been mentioned in the literature that hole diameter has a significant effect on bond strength of bolt grout interfaces (Ghazvinian & Rashidi, 2010). Figures 3 (A, B) plot the shear load versus shear displacement data obtained from resin grouted samples for different loading rates. It is clear that bond strengths at bolt-grout interface and for a loading rate of about 60 µm/min, 4115 kPa, 2948 kPa and 2400 kPa for hole diameters of 32 mm, 36 mm and 42 mm, respectively. Table 1 hence bond strength reduces by almost half if the hole diameter increases from 32 mm to 42 mm. It can also be said that irrespective of loading rate, bond strength has a decreasing trend with the increasing hole diameter for resin grouted sample. Figure 2 (A) and Figure 2 (B) shows that no along the bond strength but also the bond stiffness can reduce with hole diameter. In the latter case stiffness can reduce by almost 1/3 of its value if hole diameter changes from 32 mm to 42 mm. Hence, hole diameter must be kept as lower as possible within 32 mm for better performance of resin grouted bolts.

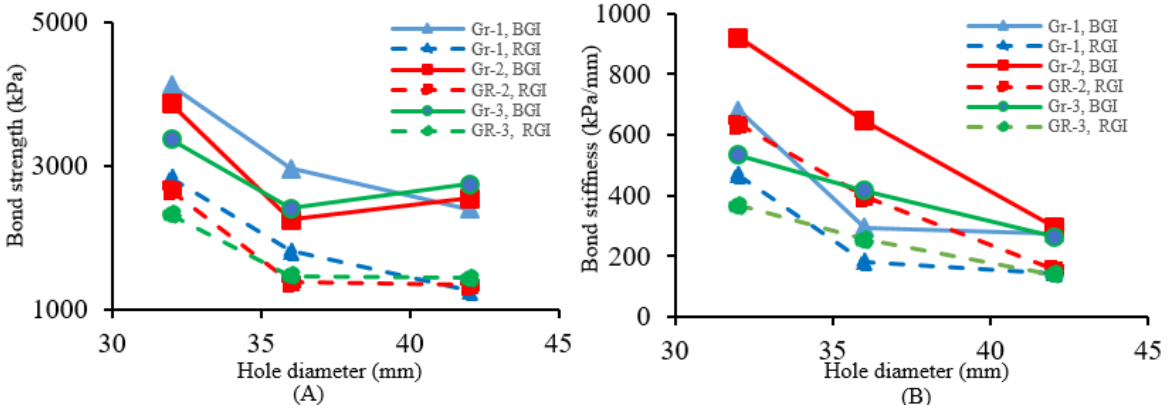

Figure 2. Bond strength versus hole diameter for different loading rates.

2.2 *Axial Strains in Bolt Rod*

Axial strains are estimated from the measured resistance data using the following equation.

$$\epsilon = \left(\frac{\Delta R}{R}\right) \times \frac{1}{SG} \tag{1}$$

Where ΔR = change of resistance, R = original or reference resistance. Here, a positive value of strain indicates tensile strains and negative value signifies compressive strain

Figures 3 (A) show the measure axial strains in four gauges for 2 representatives (Sample ID:32RG1 and 36RG2) samples. It is clear that axial strain increases with the pull load and the magnitude at strain is directly related to this load. The highest strain occurred in SG-4 strain gauge located near the loading end the lowest strain was found at SG-1. In general, axial strains in 4 gauges are higher for 32 mm hole diameter samples as compared to larger diameter samples. It is seen that axial strain recorded at gauge SG-4 (Figure 3 (B) is 0.003529 for 32 mm hole diameter sample whereas the same is 0.0018 for 36 mm hole diameter samples, respectively This indicates a substantial decrease in axial strain with hole diameter.

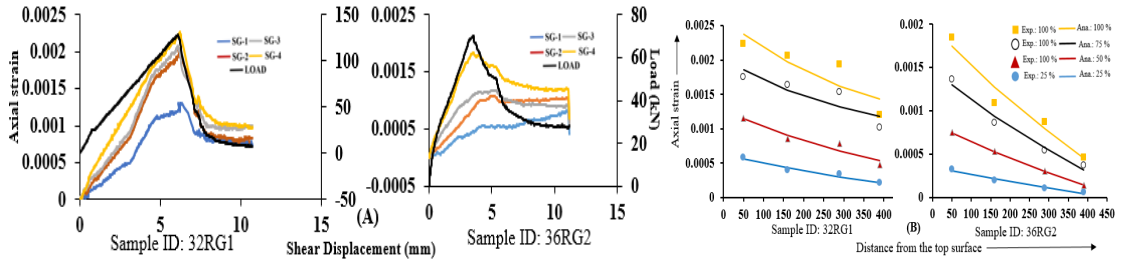

Figure 3(A). Axial Strains with Shear Displacement for resin grouted samples and
Figure 3(B). Axial strain between experimental data and the proposed analytical result.

Table 1. Bond strength and stiffness of various samples.

Sample ID	Bore hole Diameter (mm)	Loading rate (μm/min)	Peak load P (kN)	Displacement at peak load, u_p (mm) $\sigma_b = \frac{P}{\pi d_b L}$	Average Bond strength (kPa)	Average bond stiffness (kPa/mm) $\kappa = \frac{\sigma_b}{u_p}$
32RG1	32	76.7	128.0	6.04	4115.2	681.3
32RG2		160.7	120.2	4.19	3863.4	921.2
32RG3		286.6	104.7	6.32	3365.1	532.4
36RG1	36	66.5	92.2	10.06	2964.5	294.7
36RG2		183.4	69.9	3.48	2248.7	646.2
36RG3		227.9	74.8	5.80	2405.0	414.7
42RG1	42	66.2	74.7	8.77	2400.2	273.7
42RG2		205.5	79.3	8.63	2548.1	295.3
42RG3		256.8	85.4	10.42	2744.5	263.4

3 A MODIFIED ANALYTICAL SOLUTION FOR AXIAL STRAIN

3.1 *Generic Boundary Conditions*

Farmer has proposed an analytical solution of axial strain along the bolt rod, 1975 assuming two end boundary conditions as i) at $x = 0$ (loading end) pull loads is T_0 and ii) at $x = L$ (free end) axial strains is zero. Based on a given pull load, to as given below. However, in the above experiments,

pull load is applied at least 80-90 mm above the $x = 0$ point. In addition, the measured strain data clearly show that strain has also developed at $x = 390$ mm, which is close to the "free" end of the bolt. Therefore, the assumption of a strain-free boundary at $x = 450$ mm may not be appropriate for the above cases. For this reason, the boundary conditions are modified to suit the experimental results as given below constraints

i) $$\varepsilon = \frac{du_b}{dx} = \frac{\alpha T_o}{E_b A_b} \text{ at } x = 0 \tag{2}$$

ii) $$\varepsilon = \frac{du_b}{dx} = \frac{\beta T_o}{E_b A_b} \text{ at } x = L \tag{3}$$

Where T_o = measured pull load, α, β are the parameters to be determined from the measured axial strain data. With the above assumption, the bolt displacement equation becomes

$$u_b(x) = \left(\frac{\alpha T_o}{\lambda E_b A_b}\right)\left(\frac{(\beta/\alpha)\cosh(\lambda x) - \cosh(\lambda(L-x))}{\sinh(\lambda L)}\right) \tag{4}$$

It can be seen that for $\alpha = 1$ and $\beta = 0$, the above equation becomes equation Farmer's equation. Now replacing $a = \alpha$ and $b = \beta/\alpha$, the axial strain equation can be written as

$$\varepsilon = \left(\frac{aT_o}{E_b A_b}\right)\left(\frac{b\sinh(\lambda x) + \sinh(\lambda(L-x))}{\sinh(\lambda L)}\right) \tag{5}$$

3.2 Determination of Parameters α and β using Least Square Method

As mentioned, strains were measured at 4 locations along the bolt rod viz. $x = 50$ mm, $x = 160$ mm, $x = 280$ mm and $x = 390$ mm from the top surface (pulling end). These data, pull load and shear displacement were recorded at every 10 s interval. Therefore, at any given time, the sum square error between the measurement and analytical solution given via a and b equation.

$$E = \frac{1}{2}\sum_{i=1}^{4}(\hat{\varepsilon}_i - \varepsilon_i)^2 \tag{6}$$

Where, $\hat{\varepsilon}_i$ = estimated axial strain (equation 9) and ϵ_i = measured axial strain at $x = x_i$. Now by minimizing the error with respect to parameters a and b,

$$b = \frac{(\sum q_i^2)(\sum \epsilon_i p_i) - (\sum p_i q_i)(\sum \epsilon_i q_i)}{(\sum p_i^2)(\sum \epsilon_i q_i) - (\sum p_i q_i)(\sum \epsilon_i p_i)} \quad \text{and} \quad a = \frac{\sum \epsilon_i(\beta p_i + q_i)}{C\sum(\beta p_i + q_i)^2} \tag{7}$$

$$p_i = \sinh(\lambda x_i)\,, q_i = \sinh(\lambda(L - x_i)) \text{ and } C = \left(\frac{T_o}{E_b A_b}\right)\left(\frac{1}{\sinh(\lambda L)}\right) \tag{8}$$

From the values of a and b, the parameters α and β can be obtained. It may be noted that the values of α and β may change for each load increment. From the above analysis, the analytical axial strain can be determined for each load increment and is discussed in the following section.

3.3 Comparisons of Axial Strains

Once the parameters α and β are obtained, analytical axial strains at any x ranging between 0 to 450 mm can be estimated for each pull load. Figures 6 A-C compare the axial strains at $x =$

x_i between the experimental values and those estimated using equation 5 for hole diameter 32 mm, 36 mm and 42 mm, respectively for G1 and G2 category of loading rates. The data are plotted for pull load levels of 25%, 50%, 75% and 100% of the peak load. As expected, axial strain decreases nonlinearly with distance from the loading point. The proposed modified axial strain equation predicts the experimental data reasonably well. Overall RMSE error is either one or two order lower than the estimated and measured strains (in 10^{-3} range). Therefore, it can be concluded that equation estimates strains with reasonable accuracy (in 10^{-5} range) and can be used for estimating axial strain in bolt rod under pull load.This study finds that the value of α ranges between 0.2 to 0.4 and the avergae value of β is in the of 0.05

5. CONCLUSIONS

Pull test results of resin grouted instrumented rock bolts show that the borehole diameter must be kept as close to the hole diameter as possible for better performance. The study finds that for resin grouted samples, bond strength drops from 4115 kPa to 2400 kPa if the diameter of borehole increases from 32 mm to 42 mm. These results are further investigated by breaking the samples into two halves and found that resin in firm contact with the bolt rod; hence the dominant shearing surface would be rock-grout interface. Generalized equation of displacement and strain for bolt rod are derived by modifying the equation proposed by Farmer, 1975. Two new parameters α and β are introduced to make this equation more generic in nature. Based on the modified strain equation distribution of axial strains along the bolt rod is computed and compared with the measured values of 4 strain gauge locations. It is found that in most of the cases, measured values are close to the proposed analyzed solution.

REFERENCES

Benmokrane, B., Chennouf, A., & Mitri, H. S. (1995). Laboratory evaluation of cement-based grouts and grouted rock anchors. *International Journal of Rock Mechanics and Mining Sciences And*, *32*(7), 633–642. https://doi.org/10.1016/0148-9062(95)00021-8

Cai, Y., Esaki, T., & Jiang, Y. (2004). A rock bolt and rock mass interaction model. *International Journal of Rock Mechanics and Mining Sciences*, *41*(7), 1055–1067. https://doi.org/10.1016/J.IJRMMS.2004.04.005

Deb, D., & Das, K. C. (2010). Bolt-grout interactions in elastoplastic rock mass using coupled FEM-FDM techniques. *Advances in Civil Engineering*, *2010*. https://doi.org/10.1155/2010/149810

Deb, D., & Gujjala, Y. K. (2018). Extended finite element procedures for analysis of bolt crossing multiple intersecting rock joints. *International Journal of Rock Mechanics and Mining Sciences*, *107*, 249–260. https://doi.org/10.1016/J.IJRMMS.2018.04.052

Farmer, I. W. (1975). Stress distribution along a resin grouted rock anchor. *International Journal of Rock Mechanics and Mining Sciences And*, *12*(11), 347–351. https://doi.org/10.1016/0148-9062(75)90168-0

Ghazvinian, A. H., & Rashidi, M. (2010). Study of the Effect of Ratio of Hole Diameter to Rock Bolt Diameter on Pullout Capacity of Fully Grouted Rock Bolts. *Journal of Rock Mechanics and Tunnelling Tech.*, *16*(1), 11–18.

Hyett, A. J., Moosavi, M., & Bawden, W. F. (1996). Load distribution along fully grouted bolts, with emphasis on cable bolt reinforcement. *International Journal for Numerical and Analytical Methods in Geomechanics*, *20*(7), 517–544. https://doi.org/10.1002/(SICI)1096-9853(199607)20:7<517::AID-NAG833>3.0.CO;2-L

Li, C., & Stillborg, B. (1999). Analytical models for rock bolts. *International Journal of Rock Mechanics and Mining Sciences*, *36*(8), 1013–1029. https://doi.org/10.1016/S1365-1609(99)00064-7

Pinazzi, P. C., Spearing, A. J. S. (Sam., Jessu, K. V., Singh, P., & Hawker, R. (2020). Mechanical performance of rock bolts under combined load conditions. *International Journal of Mining Science and Technology*, *30*(2), 167–177. https://doi.org/10.1016/J.IJMST.2020.01.004